Pore-Tailored Hollow Mesoporous Carbon Spheres Confining Pd/PdO Nanoparticles Enable Efficient CO_2 Reduction and Propylene Oxidation Coupling

Man Zhao[‡, a], Ze Wang [‡, a], Jiamin Ma [a], Qinyun Yan[a], Liwu Qiang[a], Wei Wen[a], Lifang Shi[a], Shuai He [a], Na Gao[a], Aiqin Hao[a], Junming Zhang[a], Xiaoli Li [b, *], He Xiao [a, *], Jianfeng Jia [a, *]

[a]Shanxi Center of Technology Innovation for Advanced Power Battery Material, School of Chemistry and Chemical Engineering, Shanxi Normal University, Taiyuan, 030000, China

[b]School of Materials Science and Engineering, Hebei University of Engineering, Handan 056038, China

*Corresponding author

E-mail: lixiaoli@hebei.edu.cn (Xiaoli Li); xiaohe200808@sxnu.edu.cn (He Xiao); jiajf@dns.sxnu.edu.cn (Jianfeng Jia).

Table S1 Effect of constituent ratios on HMCs structure parameters.

Sample	H_2O/EtOH (v/v)	TPOS(mL)	Resorcinol (g)	$NH_3 \cdot H_2O$ (mL)	Pore size (nm)	S_{BET} (m^2 g^{-1})	V_{pore} (cm^3 g^{-1})
HMCs-5	10/70	0.7	0.4	3	5.06	1123.09	2.95
HMCs-10	20/60	3.5	0.4	3	10.29	1302.82	2.83
HMCs-15	40/120	6.92	0.8	6	13.05	1047.91	3.71
HMCs-20	55/110	6.92	0.8	6	18.20	1030.02	2.58

Table S2 Calculated Pd content of Pd/HMCs-x and PdO/HMCs-x based on ICP-OES.

Catalysts	Pd contents (%)	Catalysts	Pd contents (%)
Pd/HMCs-5	9.98	PdO/HMCs-5	11.34
Pd/HMCs-10	9.29	PdO/HMCs-10	11.31
Pd/HMCs-15	9.79	PdO/HMCs-15	11.99
Pd/HMCs-20	10.71	PdO/HMCs-20	13.02

Table S3 Textural parameters of HMCs and Pd/HMCs-x, PdO/HMCs-x.

Sample	S_{BET} (m^2 g^{-1})	V_{pore} (cm^3 g^{-1})	Pore size (nm)
HMCs-5	1123.09	2.95	5.06
HMCs-10	1302.82	2.83	10.29
HMCs-15	1047.91	3.71	13.05
HMCs-20	1030.02	2.58	18.20
Pd/HMCs-5	784.48	1.31	7.04
Pd/HMCs-10	800.87	1.80	10.01
Pd/HMCs-15	706.39	1.53	9.57

Pd/HMCs-20	694.06	1.97	13.28
PdO/HMCs-5	1052.90	1.61	7.53
PdO/HMCs-10	997.64	2.04	10.74
PdO/HMCs15	911.54	1.96	10.83
PdO/HMCs-20	897.27	2.25	14.06

Table S4 Comparative catalytic performance of diverse catalysts in CO_2RR.

Catalysts	Electrolyte	E (V vs RHE)	j (mA cm^{-2})	FE_{CO} (%)	Reference
Pd (3 1 0)	0.1 M $KHCO_3$	-0.90	——	90.6	[1]
CuO-IO	0.1 M $KHCO_3$	-0.60	2.5	72.5	[2]
Co-COF	0.1 M $KHCO_3$	-0.67	——	90.0	[3]
Vo-rich ZnO	0.1 M $KHCO_3$	-1.10	13.1	83.0	[4]
NiPc–MDE NTs	0.5 M $KHCO_3$	0.5	150.0	99.5	[5]
Ag@AgClxC SNWAs	0.5 M $KHCO_3$	-0.60	5.27	91.0	[6]
CuInNWs	0.5 M $KHCO_3$	-0.6	3.9	68.2	[7]
M-salophen/CNTs	0.5 M $KHCO_3$	-0.76	13.24	86.8	[8]
CoxNi1-x/N-CNFs	0.5M $NaHCO_3$	-0.90	13.40	85.0	[9]
Sn/CuNFs	0.1 M $NaHCO_3$	-0.90	100.0	80.0	[10]
Sn/N-CNFs	0.1 M $NaHCO_3$	0.69	11.0	91.0	[11]
NCNTs	0.1 M $NaHCO_3$	-0.26	——	80.0	[12]

Pd/HMCs-10	0.5 M $KHCO_3$	-0.60	12.0	85.5	This work

Table S5 Comparative catalytic performance of diverse catalysts in POR.

Catalysts	Electrolyte	Electric voltage	j	FE (%)	Reference
PdC	0.1M $HClO_4$	1.4 V vs. RHE	2.5(mA mg^{-1}_{Pd})	— PG	[13]
PdO/C	0.1M $HClO_4$	1.4 V vs. RHE	0.49(mA mg^{-1}_{Pd})	— PG	[13]
Pd Electrode	1 M HClO4	1.2 V vs RHE	0.2(mA cm^{-2})	— PG	[14]
Pd Oxide	phosphate buffer	1.2 V vs RHE	——	——	[14]
Ru-Pd	0.1 M ClO_4^-	1.1 V vs Ag/AgCl	——	20(PG)	[15]
Ag-Pd	0.1 M ClO_4^-	1.1 V vs Ag/AgCl	——	40(PG)	[15]
PdPtOx/C	0.1M PBS +ACN	1.2 V vs RHE	50(mA cm^{-2})	66±5(PO)	[16]
Ag-V-O/GDL	0.1M PBS	1.0 V vs Ag/AgCl	10(mA cm^{-2})	30.4(PO)	[17]
Ag_3PO_4	0.1M PBS	2.2 V vs RHE	0.49(mA cm^{-2})	18.7(PO)	[18]
PdO/HMCs-10	0.1 M PBS	1.6 V (vs. Ag/AgCl)	4.0(mA cm^{-2})	47.11(PO)	This work

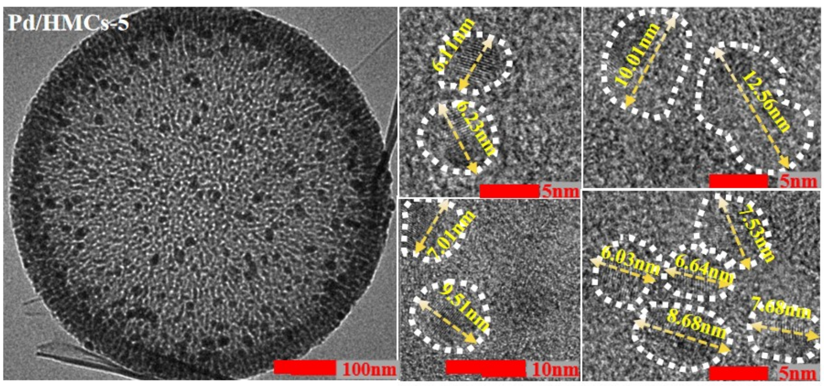

Fig. S1 HRTEM images of as-prepared Pd/HMCs-5 samples.

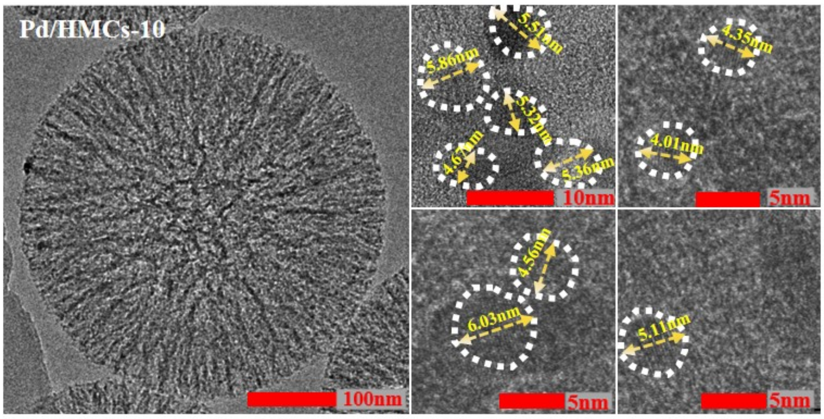

Fig. S2 HRTEM images of as-prepared Pd/HMCs-10 samples.

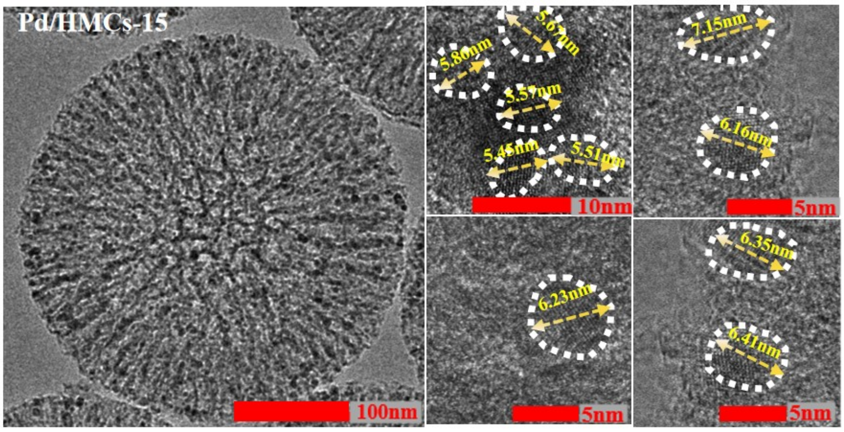

Fig. S3 HRTEM images of as-prepared Pd/HMCs-15 samples.

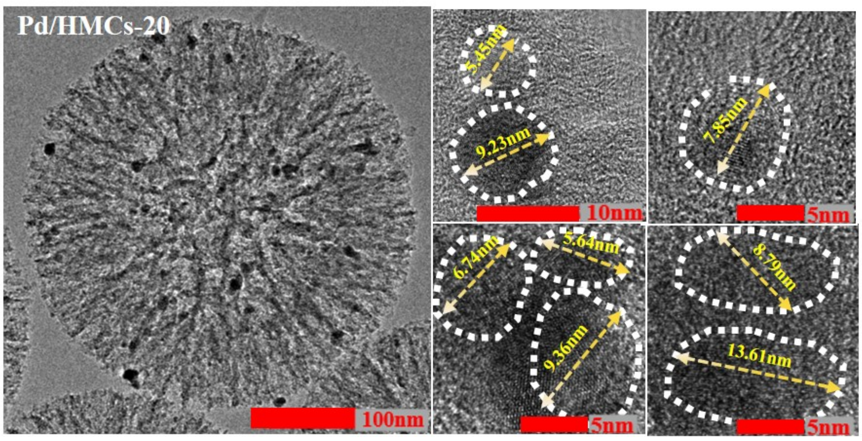

Fig. S4 HRTEM images of as-prepared Pd/HMCs-20 samples.

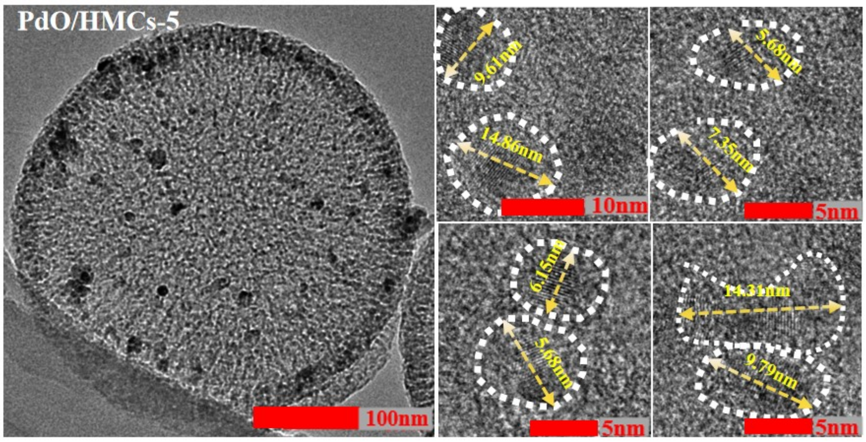

Fig. S5 HRTEM images of as-prepared PdO/HMCs-5 samples.

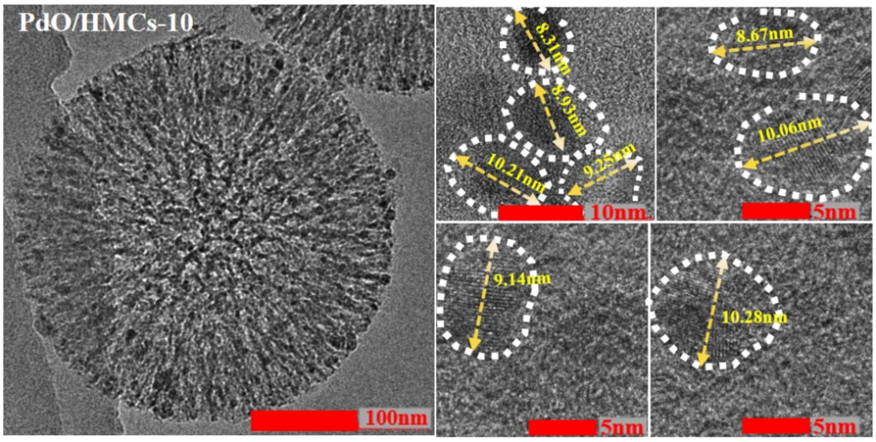

Fig. S6 HRTEM images of as-prepared PdO/HMCs-10 samples.

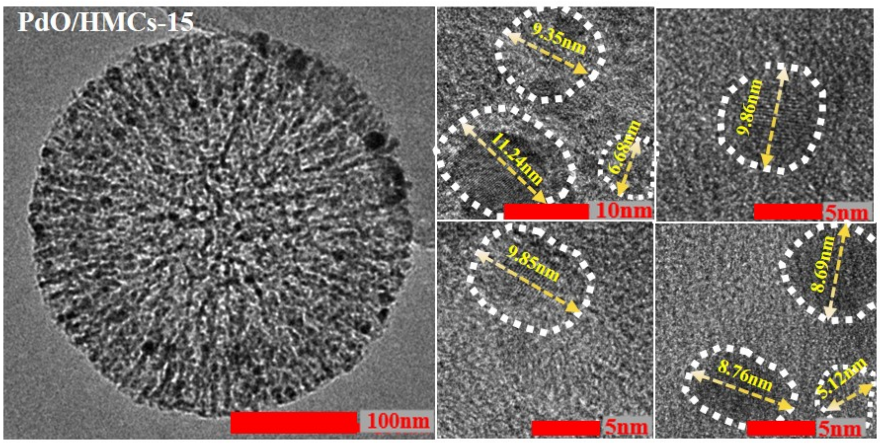

Fig. S7 HRTEM images of as-prepared PdO/HMCs-15 samples.

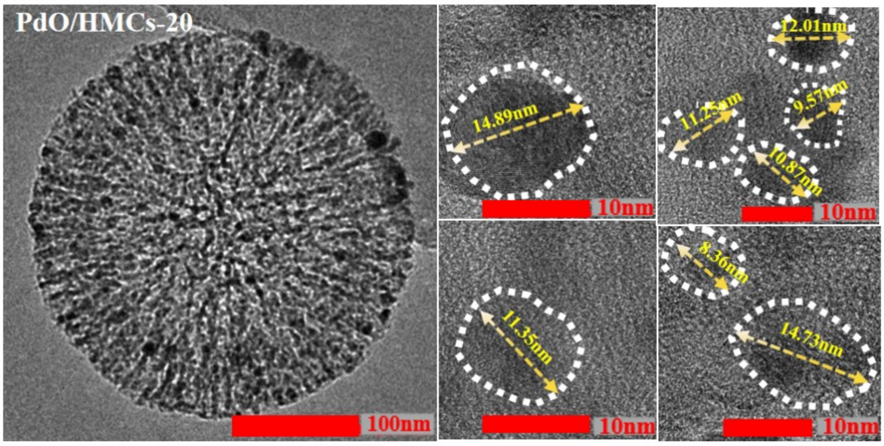

Fig. S8 HRTEM images of as-prepared PdO/HMCs-20 samples.

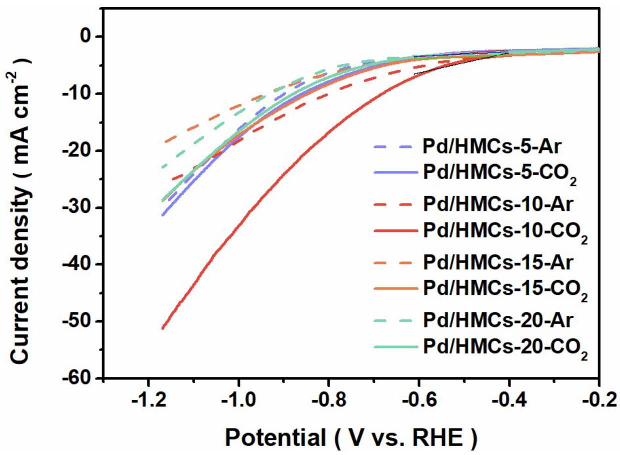

Fig. S9 LSV curves of Pd/HMCs-x in Ar/CO_2-saturated 0.5 M $KHCO_3$.

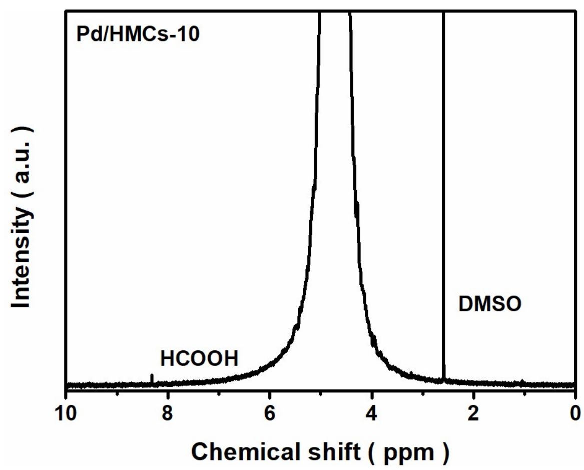

Fig. S10 ^{1}HNMR spectra of Pd/HMCs-10.

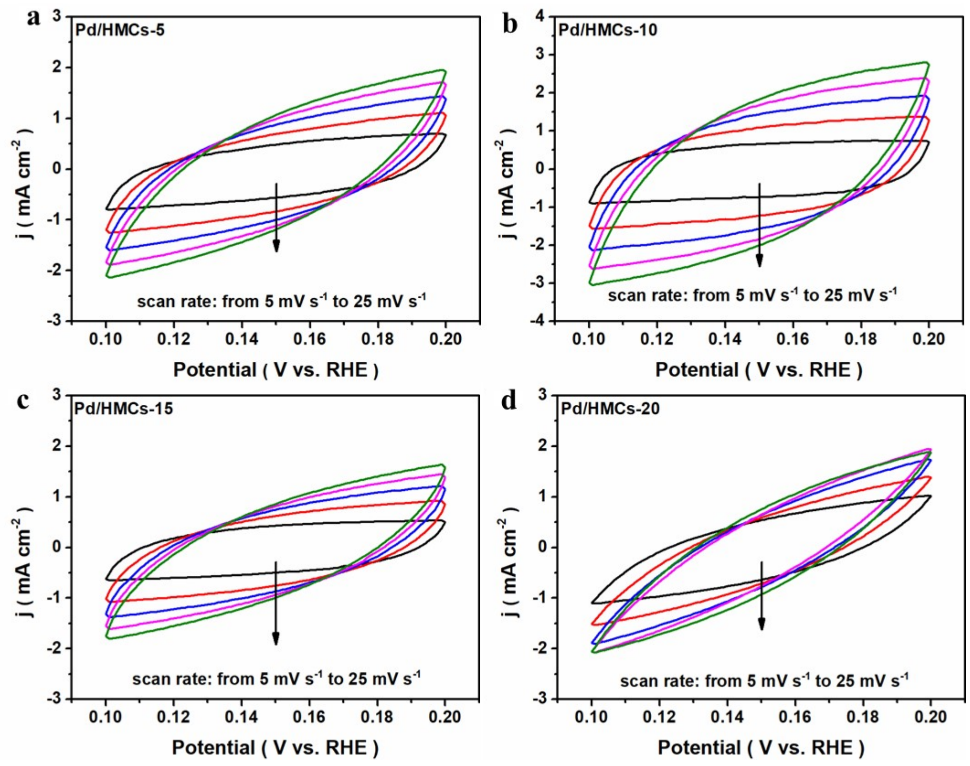

Fig. S11 Cyclic voltammetry curves at scan rates from 5 to 25 mV·s^{-1} of Pd/HMCs-x.

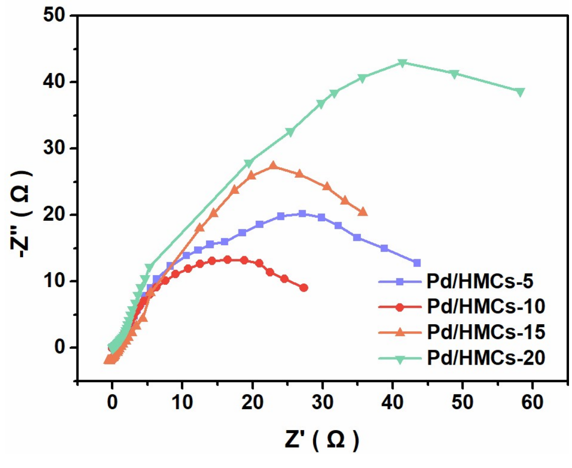

Fig. S12 EIS curves of Pd/HMCs-x.

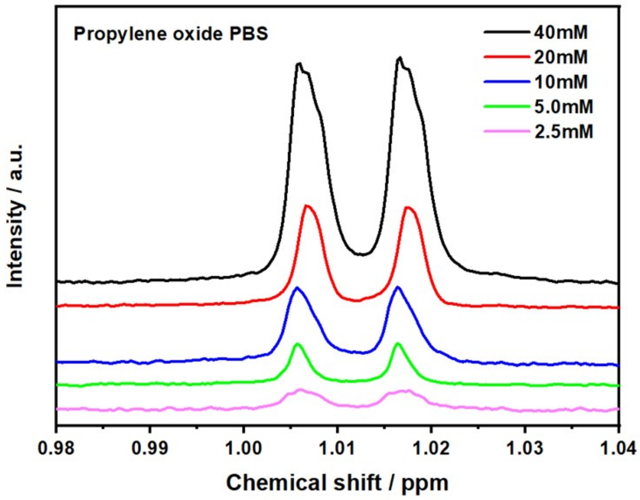

Fig. S13 ^{1}H NMR spectra of different concentrations propylene oxide.

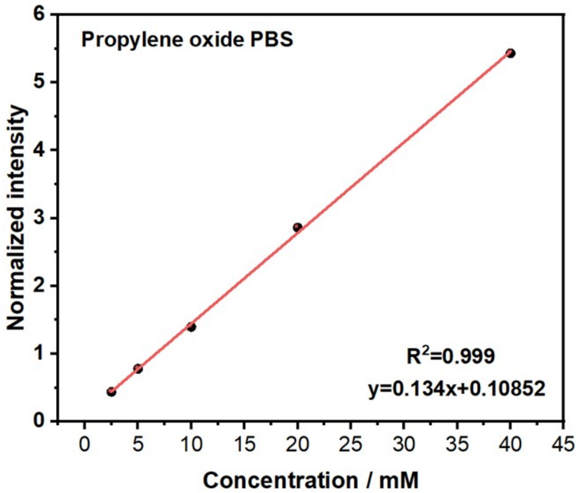

Fig. S14 Standard curve for propylene oxide.

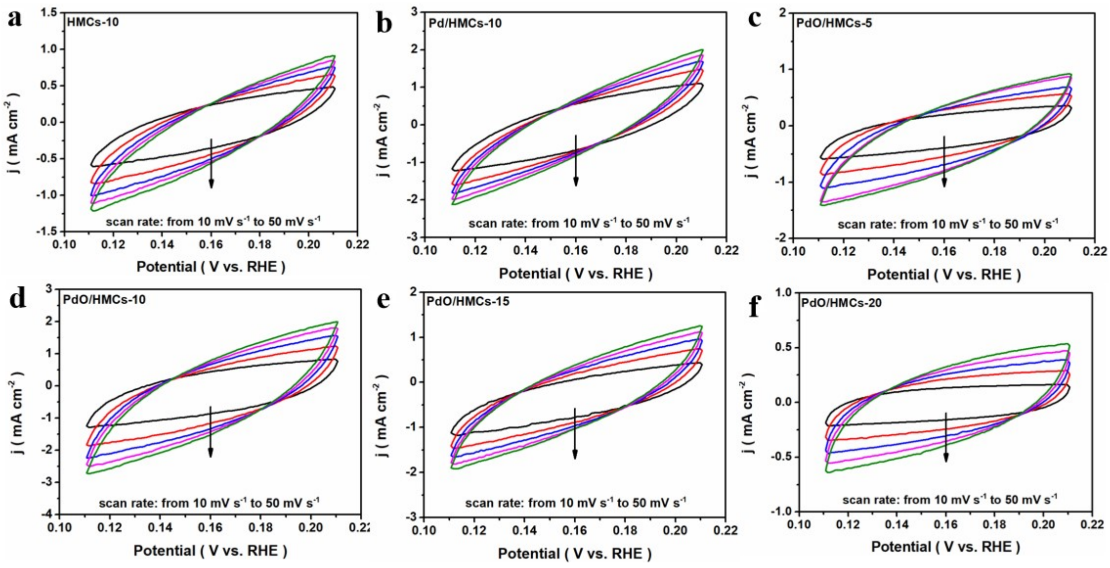

Fig. S15 Cyclic voltammetry curves of HMCs, Pd/HMCs-10 and PdO/HMCs-x at scan rates from 10 to 50 mV·s^{-1}.

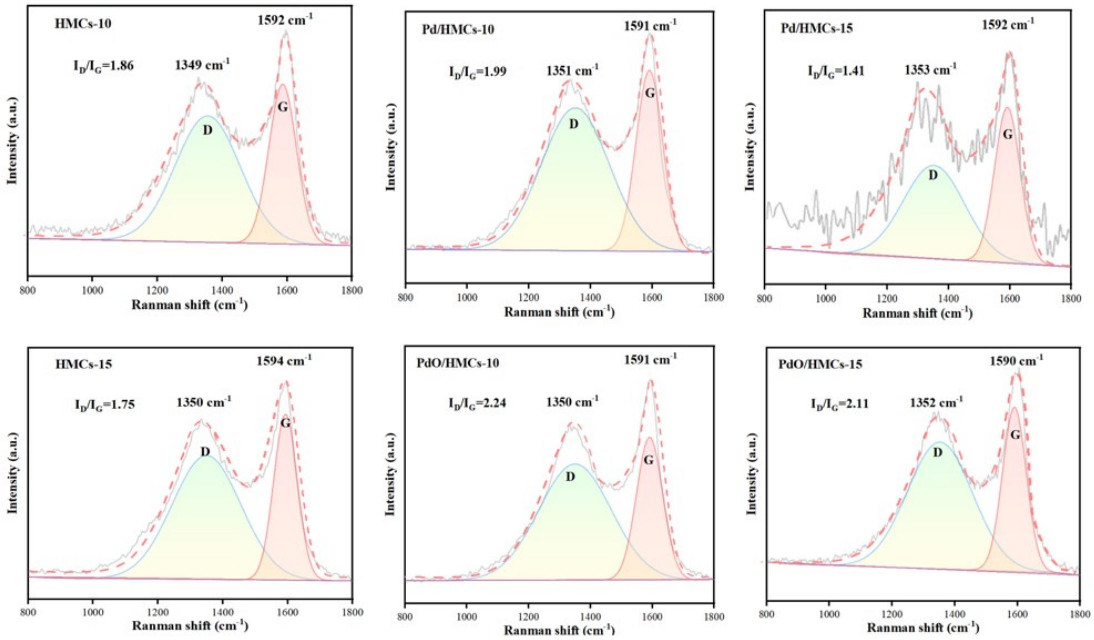

Fig. S16 Raman spectra of (a) HMCS-10, (b) Pd/HMCS-10, (c) PdO/HMCS-10, (d) HMCS-15, (e) Pd/HMCS-15, (f) PdO/HMCS-15.

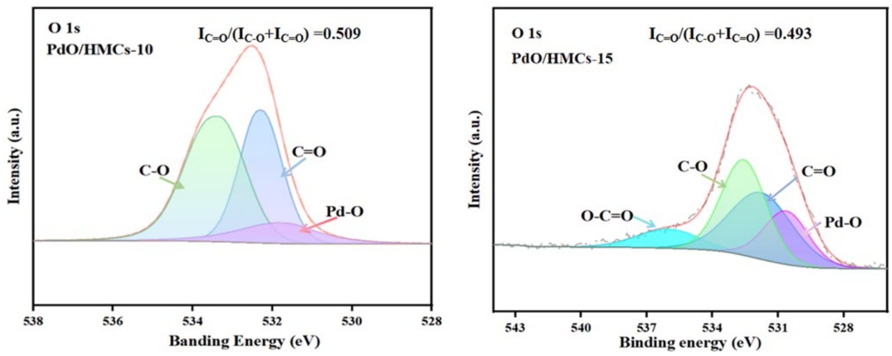

Fig. S17 O 1s XPS spectra of PdO/HMCs-10 and PdO/HMCs-15 samples.

References

1 H. Dong, L. Zhang, P. Yang, X. Chang, W. Zhu, X. Ren, Z.-J. Zhao and J. Gong, *Chemical Engineering Science*, 2019, **194**, 29-35.

2 T.-D. Nguyen-Phan, C. Wang, C. M. Marin, Y. Zhou, E. Stavitski, E. J. Popczun, Y. Yu, W. Xu, B. H. Howard, M. Y. Stuckman, I. Waluyo, P. R. Ohodnicki and D. R. Kauffman, *J. Mater. Chem. A*, 2019, **7**, 27576-27584.

3 S. Lin, C. S. Diercks, Y.-B. Zhang, N. Kornienko, E. M. Nichols, Y. Zhao, A. R. Paris, D. Kim, P. Yang, O. M. Yaghi and C. J. Chang, *Science*, 2015, **349**, 1208-1213.

4 Z. Geng, X. Kong, W. Chen, H. Su, Y. Liu, F. Cai, G. Wang and J. Zeng, *Angew. Chem. Int. Ed.*, 2018, **57**, 6054-6059.

5 X. Zhang, Y. Wang, M. Gu, M. Wang, Z. Zhang, W. Pan, Z. Jiang, H. Zheng, M. Lucero, H. Wang, G. E. Sterbinsky, Q. Ma, Y.-G. Wang, Z. Feng, J. Li, H. Dai and Y. Liang, *Nat. Energy*, 2020, **5**, 684-692.

6 J. Ge, J. Long, Z. Sun, H. Feng, J. Hu, S. W. Koh, Q. Yu, J. Xiao and H. Li, *ACS Appl. Energy Mater.*, 2019, **2**, 6163-6169.

7 Y. J. Jang, J. Lee, J. H. Kim, B. J. Lee and J. S. Lee, *J. Power Sources*, 2018, **378**, 412-417.

8 X. Cui, S. Liu, L. Zhao, J. Yu, S. Ling, Y. Zhao, J. Wang, W. Qin, X. Mao and J. Zhang, *J. Colloid Interface Sci.*, 2022, **608**, 1827-1836.

9 W. Zhang, J. Zeng, H. Liu, Z. Shi, Y. Tang and Q. Gao, *Journal of Catalysis*, 2019, **372**, 277-286.

10 W. Ju, F. Jiang, H. Ma, Z. Pan, Y.-B. Zhao, F. Pagani, D. Rentsch, J. Wang and C. Battaglia, *Advanced Energy Materials*, 2019, **9**, 1901514.

11 Y. Zhao, J. Liang, C. Wang, J. Ma and G. G. Wallace, *Advanced Energy Materials*, 2018, **8**, 1702524.

12 J. Wu, R. M. Yadav, M. Liu, P. P. Sharma, C. S. Tiwary, L. Ma, X. Zou, X.-D. Zhou, B. I. Yakobson, J. Lou and P. M. Ajayan, *ACS Nano*, 2015, **9**, 5364-5371.

13 X.-C. Liu, T. Wang, Z.-M. Zhang, C.-H. Yang, L.-Y. Li, S. Wu, S. Xie, G. Fu, Z.-Y. Zhou and S.-G. Sun, *J. Am. Chem. Soc.*, 2022, **144**, 20895-20902.

14 R. P. H. Jong, E. Dubbelman and G. Mul, *Journal of Catalysis*, 2022, **416**, 18-28.

15 J. E. Huang, Y. Chen, P. Ou, X. Ding, Y. Yan, R. Dorakhan, Y. Lum, X.-Y. Li, Y. Bai, C. Wu, M. Fan, M. G. Lee, R. K. Miao, Y. Liu, C. O'Brien, J. Zhang, C. Tian, Y. Liang, Y. Xu, M. Luo, D. Sinton and E. H. Sargent, *J. Am. Chem. Soc.*, 2024, **146**, 8641-8649.

16 M. Chung, J. H. Maalouf, J. S. Adams, C. Jiang, Y. Román-Leshkov and K. Manthiram, *Science*, 2024, **383**, 49-55.

17 Y. Lin, H. Li, X. Miao, Y. Sun, H. Ren, X. Yu, W. Cui, M. Wu and Z. Li, *Nat. Commun.*, 2025, **16**.

18 J. Ke, J. Zhao, M. Chi, M. Wang, X. Kong, Q. Chang, W. Zhou, C. Long, J. Zeng and Z. Geng, *Nat. Commun.*, 2022, **13**, 932.